

## Drop Diameter Prediction Model for Liquid Phase Dispersion In A Supersonic Nozzle with Wet Steam Flow

*Dr. Hussein Wheeb Mashi and Dr. Samir Ali Alrabii  
University of Technology  
Mechanical Eng. Dep.*

### ABSTRACT

*This paper is an attempt to obtain a prediction model for the drop diameter for the liquid phase dispersion in a supersonic nozzle with wet steam. The dispersion of liquid phase and gas dynamic characteristics of the flow of wet steam in Laval nozzles were first studied. A measuring method for dispersion was applied for subsonic and supersonic speeds. A single channel with a model that approximates to what exists between the turbine blades (Laval Nozzle) with different dimensions was designed. An optical unit was also designed on the basis of the work within the small angles method. At the end of the measuring processes for the intensity of the scattered light by laser scattering small angles method, the drop diameter was calculated and all results were analyzed using "DESIGN EXPERT 8" experimental design software. The experimental design used was based on the response surface methodology (RSM) using a central composite design (CCD). A mathematical model of the response (drop diameter) as function of the conditions used (light intensity, pressure ratio, and moisture ratio) was obtained and studied.*

*It is found that the calculated diameter of the drops of the condensed steam along the longitudinal axis of the channel varies between (40-110 $\mu$ m) according to the pressure ratio change. Also, the diameter of the steam drops is within (40-110 $\mu$ m) according to the variation of the moisture ratio that, where the error is not more than (15%). The geometry of Laval nozzle has a great influence on the nature of the flowing steam through the channel (diameter of drops, compressive shock). The resultant predicted two-factor interaction (2FI) model with a 95% confidence level showed that the pressure ratio, the interaction of pressure ratio and moisture ratio, and their squares were significant terms. According to the results obtained, the predicted model indicated that both pressure ratio and moisture ratio had a significant effect on drop diameter, but pressure ratio had the highest impact, whereas, variation of the light intensity factor had insignificant influence on drop diameter.*

**Key words:** Wet steam, Droplet diameter, Pressure ratio, Moisture ratio, light intensity  
Laser scattering small angles method, Supersonic nozzle.

## الخلاصة

يعتبر هذا البحث محاولة لإيجاد تشتت وخصائص ديناميك الغاز لجريان البخار الرطب في فوهات لافال (قنوات معينة لسرع دون وفوق سرعة الصوت). تم تطبيق طريقة قياس للتشتت لسرع دون وفوق الصوتية. وتم تصميم قناة أحادية مع نموذج مشابه لما موجود بين ريش التوربين (قناة لافال) بأبعاد مختلفة. كما تم تصميم وحدة ضوئية على أساس العمل بطريقة الزوايا الصغيرة. بعد الانتهاء من عمليات قياس شدة الضوء المشتت بطريقة التشتت الليزرية للزوايا الصغيرة، تم حساب قطر القطرات وتحليل جميع النتائج باستخدام برنامج (DESIGN EXPERT 8) للتصميم التجريبي. أستند التصميم التجريبي المستخدم على منهجية سطح الاستجابة (RSM) باستخدام تصميم مركب مركزي (CCD). تم إيجاد ودراسة النموذج الرياضي للاستجابة (قطر القطرات) بدلالة الظروف المستخدمة (شدة الضوء، نسبة الضغط، نسبة الرطوبة). ووجد أن قطر قطرات البخار المتكثف على امتداد المحور الطولي للقناة يتغير بين (40-110) ميكرومتر وفقا الى نسبة تغير الضغط. ويتراوح أيضا قطر قطرات البخار بين (40 - 110) وفقا الى تغير نسبة الرطوبة، حيث ان نسبة الخطأ لا تزيد عن 26%. كما أن للشكل الهندسي لفوهة لافال تأثيرا كبيرا على طبيعة البخار الجاري خلال القناة (قطر القطرات والصدمة الانضغاطية). وأظهر النموذج المنبأ الناتج ذو العوامل الثنائية التداخل (2FI) مع 95% مستوى ثقة بأن نسبة الضغط وتداخل نسبة الضغط مع نسبة الرطوبة ومربعاتها عوامل مهمة فيه. ووفقا للنتائج المتحصلة، بين النموذج المنبأ بان كل من نسبة الضغط ونسبة الرطوبة كان لهما تأثير مهم على قطر القطرات، ولكن نسبة الضغط لها التأثير الاعلى. بينما لم يكن لتغيير عامل شدة الضوء تأثيرا مهما على قطر القطرات.

## INTRODUCTION

Condensation occurs and droplets grow in the nozzle (fixed blades) of the last stage of steam turbine and in the low-pressure steam turbine stages [1]. The condensation process consists of two consecutive stages: the formulation of liquid nuclei (nucleation) and the condensation of vapor molecules on the already present nuclei (droplet growth).

It is known that in the turbine flows, some droplets form by a heterogeneous condensation on the impurities present in the steam. However, such droplets are relatively few in number and grow to a sufficient size so as to quickly deposit on the wall and blades. Thus, the steam becomes super-cooled with further expansion such that the homogeneous nucleation is usually the dominant mechanism [2]. These droplets cause an efficiency reduction of the turbine because the shock condensation occurs, which rises the static pressure. Therefore, droplet size measurements are necessary in order to accurately estimate and reduce the mechanical and thermodynamic losses [1].

Several studies of droplet size measurements have been recently made in steam turbines (nozzles and blades). In these measurements, the forward scattering method [1], the side scattering method [3,4] and light extinction method [4] were used.

In the light extinction method, the transmission of a monochromatic light, measured at several wavelengths, is inverted to yield the droplet size distribution using the following equation:

$$T(\lambda) == \exp[-L \int C(\lambda, D)n(D)dD] \quad \dots\dots\dots (1)$$

Where,

$T(\lambda)$  = transmission ratio of monochromatic light with  $(\lambda)$ .

$L$  = scattering path length, m.

$C(\lambda, D)$  = extinction cross section,  $m^2$ .

$\lambda$  = light wavelength,  $\mu m$ .

$D$  = average droplet diameter,  $\mu m$ .

$n(D)$  = number of droplet in scattering path length.

The advantages of this method is that, if the droplet density is low,  $T(\lambda)$  is larger than (0.9), therefore, the variation of  $T(\lambda)$  with  $(\lambda)$  is very small. In this case, it is very difficult to determine the droplet size distribution using equation (1). Also, droplets larger than (2 $\mu m$ ) in diameter cannot be measured if  $\lambda$  is in the visible light rang because  $C(\lambda, D)$  is only a function of  $(D)$  for ( $\pi D/\lambda \geq 10$ ).

In the side scattering method, the droplet size is determined from the scattered light pulse height. In this method, the scattering zone has to be small so that it contains zero or one particle. Therefore, this method is not applicable to measurements in the case of high droplet densities.

The forward scattering method measures the scattered light density pattern by many particles and inverts it to a droplet size distribution using equation;

$$I(\theta) = \int i(D, \theta) n(D) dD \quad \dots\dots\dots (2)$$

Where,

$I(\theta)$  = scattered light intensity pattern by measured droplet.

$i(D, \theta)$  = scattered light intensity by  $D$  and  $n$  diameter.

$\theta$  = scattering angle, deg.

This method is applicable to droplets at a high density and has a wide measurable range.

In order to raise the performance of the turbines that work with a wet steam, a detailed investigation for the hydro-gas dynamics in the turbine blade at a wet steam is necessary to decrease the losses due to the humidity and to increase the safety degree from erosion.

The results of previous studies [1-18] do not allow solving some problems, especially those concerned with supersonic speeds at the last stages of the steam power turbines. Accordingly, this research appears to be important to carry out, particularly, a measuring method for dispersion was applied for subsonic and supersonic speeds. Also, the goal of the present work is to obtain the dispersion and the gas dynamic characteristics of the wet steam flow in Laval nozzles.

## METHODOLOGY

- 1- Designing a single nozzle model that approximates to those supersonic nozzles which exist between the turbine blades. And, this nozzle was used to conduct the experiments for a wide range of wet steam systems listed in **Table 1**.
- 2- Designing an optical unit on the basis of working by a small angle method which allows measuring both the liquid phase drops at different steps of dispersion and the local relative humidity in the nozzle for various systems.
- 3- Confirming the interaction of the drops with the compressive wave in the non calculated working systems for the channel, and predicting the intensity of the formation of shock condensation on the location (position) in the divergent part of the nozzle.
- 4- Obtaining the detailed characteristics for the single distinguished phase along the nozzle axis and its cross-section at different humidity steps for the working nozzle of various geometries.
- 5- Defining the location of the mean of the relative humidity in the nozzle.

## Laser Scattering Small Angles Method

This method is based on measuring the intensity of the scattered light within small angles distributed in a conical shape along the principal light beam. These encompassed or subtended angles are between (0-22°) and normally used to determine the diameter of the surrounded steam drops between (2-300 $\mu$ m) through transmission of a monochromatic light beam with a wavelength of ( $\lambda = 0.632\mu$ m), such as laser, neon, and helium (He-Ne). The transmitted light scatters through condensed water from the steam at very small angles with a little divergent that permits illuminating a small size of the two-phase median. The light intensity scattered through a spherical droplet with a diameter ( $r$ ) can be calculated by Mie theory [11], and is expressed by  $I(r, \gamma, m, \lambda)$  as a function of ( $r, \gamma, m, \lambda$ ).

The intensity of the scattered light is first measured in case of no steam exists ( $I_0$ ) in which the falling laser beam is perpendicular to the flow direction. Then, the light intensity is measured in a similar previous method but with steam existence which is denoted by the symbol [ $I(\gamma)$ ]. The He-Ne laser beam is

led to scattering through the nozzle. This parallel beam is directed at the measured droplets in the scattering zone, and scattering by the spherical droplets the scattered light is received by photoelectric cell. The readings of microampere device are used in a computer program using the equations relevant to the mentioned method for obtaining the drops diameter, density, and moisture percentage in the illuminated unit size.

**Calculation Method of Drop Diameter**

Prior to measuring, the optical instruments are set, and initial flow conditions are specified (P<sub>o</sub>,T<sub>o</sub>) for the two-phase median. At the beginning of calculation, the falling beam intensity (I<sub>o</sub>) is taken as a constant and then plotted as a curve for the relation between (I<sub>o</sub>) and (γ). The light is measured in case of steam existence by a primary given values to the curve for I(γ) and (γ) relationship. The average of the transmitted beam intensity value [I(γ)] is taken as shown in **Fig,(1)**. Where, (γ) represents the encompassed measuring angle between (0-22°) and measured within tables that present (w =ργ) with values of (w = 0-10) and a step of (Δw = 0.1). The density of the steam (ρ) is calculated according to this equation:ρ = 2πr/λ. And, there is a relation between f(ρ) = I(γ)/I<sub>o</sub> which is the basis of constructing the tables in the Appendices. As the (γ) changes, the function f(ρ) changes also, where ρ = constant.

When a monochromatic light beam with a wavelength value of (λ) transmitting through a two-phase median, the specifications of the particle distribution predict the diameter of the drop according to this function: f(r) = dn/dr. Where, n is the no. of particles in the illuminated size (or volume), and r is the diameter of the steam drop. And, the intensity of the transmitted light from a small angle (γ) is determined by the integral relation:

$$I(\gamma) = \frac{I_0}{\gamma^2} \int_0^\infty f(r) r^2 I_1^2(\rho\gamma) dr \dots\dots\dots (3)$$

$$f(r) = \frac{2}{\rho^2} \int_0^\infty f(\rho\gamma) \phi(\gamma) d\gamma \dots\dots\dots (4a)$$

$$f(r) = \frac{C^*}{2} \int_0^\infty f(\rho\gamma) \phi(\gamma) d\gamma \dots\dots\dots(4b)$$

$$f(\rho\gamma) = \gamma I(\rho\gamma) Y(\rho\gamma) \dots\dots\dots (5)$$

$$\phi(\gamma) = \frac{d}{d\gamma} \left[ \gamma^3 \frac{I(\gamma)}{I_0} \right] \dots\dots\dots (6)$$

$$C^* = 1/2 (\lambda/\pi)^2 \dots\dots\dots (7)$$

Where,

I(ργ)=Bessel function first order.

Y(ργ)=Bessel function second order.

ρ=2πr/λ- parameter of diffraction.

By using the above mentioned equations, the output are predicted from the experiment for the intensity of the transmitted light  $I(\gamma)$  at small angles of  $(\gamma)$ , and the graphical relation is shown in **Fig.(2a)**. This graphical plot can be established between  $f(\gamma) = \bar{I} = [ I(\gamma) / I_0(\gamma) ] * \gamma^3$  and the angle  $(\gamma)$  as shown in **Fig.(2b)**. Then, determine  $\phi(\gamma) = d/d\gamma [ I(\gamma) / I_0(\gamma) ]$  [see **Fig.(2c)**]. To know the value of  $\rho(r)$ , the function under the integration is calculated by equation (4) and the table attached to obtain the values of  $f(\rho\gamma)$ . Also, the graphical plot [**Fig.(2c)**] can be used to calculate the value of  $(r)$  by determining equation (4). As result, the relation  $C * f(r)$  is obtained as shown in **Fig.(2d)**, and the relation  $C * r^3 f(r)$  is depicted in **Fig.(2e)**. These curves represent the equations for integrations:  $\int_0 C * (r)dr$  and  $\int_0 C * r^3 (r) dr$ . Finally, the distribution curve for the drop size  $f^-(r)$  is obtained as shown in **Fig.(2f)** and then the mass by distribution  $r^3 f^-(r)$  as illustrated in **Fig.(2g)**.

When using the small angles method, the following must be verified:

- 1- The drop concentration in the unit of the measured size must not be very high. An exception for that, the secondary transition within the following limit:  $(r/d \ll 1)$  when  $(d)$  is the distance between the drops that have the diameter  $(r)$ .
- 2- The optical thickness of the illuminated part  $(\delta)$  is limited by the following equation:  
 $\delta = \ln I_0 / I_0(\gamma)$ , and the value of  $(\delta)$  must be more than  $(\delta = 0.3)$  where  $I_0$ -scattering in the air , $I_0$ -scattering in the steam.

## Response Surface Methodology

Response surface methodology (RSM) is a collection of mathematical and statistical techniques that are used for empirical model building and analysis of problems, in which a response of interest is influenced by several variables, and the objective is to optimize this response [5-6]. It has been extensively used in different engineering applications and fields. RSM is important in designing, formulating, developing, and analyzing new scientific studying and products. It is also efficient in the improvement of existing studies and products. The application of RSM to design optimization is aimed at reducing the cost of expensive analysis methods (e.g., finite element method or CFD analysis) and their associated numerical noise. By careful *design of experiments*, the objective is to optimize a *response* (output variable) which is influenced by several *independent variables* (input variables). An experiment is a series of tests, called *runs*, in which changes are made in the input variables in order to identify the reasons for changes in the output response. The advantages of design of experiments, as reviewed by Aggarwal and Singh [7], are as follows: (1) Numbers of trials are reduced. (2) Optimum values of parameters can be determined. (3) Assessment of experimental error can be made. (4) Qualitative estimation of parameters can be made. (5) Inference regarding the effect of parameters on the characteristics of the process can be made.

## Experimental design and testing

The input parameters used in the whole experimentation were selected according to the practical experience and the limitations of the measuring of the light scattering plant. These factors are given in

**Table 2** with three levels. The experimental design used was the response surface methodology using a central composite rotatable design for  $2^3$  factors, with 6 central points and  $\alpha = \pm 2$ . 20 tests were performed according to the experimental design matrix (*6 center points*). The tests were performed at random using the run order listed in **Table 3**. Each parameter was tested at different code levels of  $-2, -1, 0, +1,$  and  $+2$ , whereby each level tested conformed to an actual value equivalent to the coded value.

Thus, the input parameters studied are light intensity ( $I_0$ ), pressure ratio ( $\epsilon_0$ ) and moisture ratio ( $Y_0$ ). The experimental design matrix used for input parameters in terms of actual factors with the experimental values of average drop diameter is given in **Table 4**. The software DESIGN EXPERT 8 was used to develop the model. Results of test runs are reported, as well as, the prediction model produced within a 95% confidence interval.

## EXPERIMENTAL WORK

### Design of the Model

A single channel with a model that approximates to what exists between the turbine blades, with different dimensions was designed. The work of this design was conducted in Moscow P.E.I. The design of three channels with various lengths where the ratio of the pressure  $\epsilon_0 = P_a/P_0$  is as follows: (0.238, 0.242, 0.245) with width of (40 mm) and Mach number of (1.63, 1.602 1.63). And, these channels exhibit the effect of the geometry on the specifications by using different values of pressure ratio ( $\epsilon_0$ ) which falls within the range (1, 2, 3) as well as using various ratios of moisture ( $Y_0$ ).

### Design of an Optical Unit

An optical unit was designed on the basis of the work within the small angles method that permits measuring the diameter of the condensed steam drops in a range of (2-300 $\mu$ m) by which the moisture percentage of the flowing material can be predicted as shown in **Fig.(3)**. The optical unit consists of (He-Ne Laser,  $\lambda=0,632\mu$ m visible ray, photoelectric cell K-51, high voltage source BCB-1, Micro ampere (ammeter) K-M95, 10 $\mu$ A, 11 $\Omega$ , Show device K-M95, Variable opening, Working body, Nozzles, Shady device K-EAB-451, Mechanical device).

### Determination of Pressure Distribution

In this research, the composition of the flowing steam (supplied from a boiler as a superheated ) through Laval channel from can get three phases (dry, wet, and superheated) and several moisture ratios (by increasing or decreasing of water mass in the flowing steam using a control valves) were carried out. The relation between the diameter of drops ( $\mu$ m) and the channel length is plotted to show the diameter of drop distribution inside the channel along its longitudinal axis (mm) and for different pressure ratios and different moisture ratio for channel N1A , **Fig.(4)**.



Similarly, for the other two channels, the diameter of drops was determined for these channels at a constant moisture ratio and several various pressure ratios. Also, the diameter of drops was indicated at a constant pressure ratio ( $\epsilon_0$ ) with different values of moisture ratio.

### Measuring Procedure

At the beginning of the measuring to calculate the diameter of the steam drops, the followings have been performed:

- 1- Measuring the intensity of the falling beam that passed through before the steam being exist ( $I_0$ ).
- 2- Setting the initial parameters ( $Y_0, P_0, T_0$ ) for the flowing steam. The temperature was measured by a thermometer, and the pressures of steam were measured by a pressure gauge. These pressures were controlled by a vacuum system to determine the pressure ratio.
- 3- Measuring the intensity of the laser beam of the existence of the steam  $I(\gamma)$  within the held flowing conditions.
- 4- Measuring the intensity of the beam for different angles that exist between (1-22) in one degree step.
- 5- Measuring the intensity of the transmitted beam (through the model) in regions that positioned along the longitudinal axis between (13-20) positions.
- 6- In case of fixing a certain ratio of moisture, the results for different values of pressure ratio are calculated, such as in the channel (NIA), the moisture ratio is ( $Y_0 = 9.75\%$ ).
- 7- Setting the pressure ratio at ( $\epsilon_0 = 0.574$ ), and the results are obtained with different values of pressure ratio ( $Y_0 = 4.6\%, 6.8\%,$  and  $9.75\%$ ).

### RESULTS AND DISCUSSION

The measuring result obtained in the channel (NIA) at a moisture ratio of (4.6%) indicates following. The drops diameter varies within ( $r = 40\mu\text{m}$ ) and ( $r = 90-100\mu\text{m}$ ), and this means that the drop size is limited by the nature of the pressure ratio and flowing steam conditions from the existence of the shocks or not. When the drops diameter has a large value the ( $\epsilon_0 = 0.74$ ), there is increase in the diameter more than the another value of ( $\epsilon_0 = 0.54, 0.60, 0.66$ ). Therefore, diameter drops dependent on the pressure ratio more than the another factors because the coagulation process take more time with subsonic ( $\epsilon_0 = 0.74$ ) flow in the nozzle. The diameter drops increases along the X-axis in the convergent-divergent parts and in the cross section of the nozzle. Different ratios of pressure have been investigated for the same magnitude of moisture ( $\epsilon_0 = 0.54, 0.60, 0.66,$  and  $0.74$ ), as shown in **Fig. (4)**.



In the N1A channel and by selecting another value for moisture ratio, as the moisture ratio continues to increase up to  $Y_o = 9.75\%$  by using different values of pressure ratios ( $\epsilon_a = 0.54, 0.60, 0.66$  and  $0.74$ ), the initial values of the average radius of the droplet ( $r \approx 60 \mu\text{m}$ ) and ( $r=90-130 \mu$ ) increase in the adjacent part of the nozzle with continual increase in the average radius of droplets with steam flowing toward the channel exit as in the above case, and as shown in

**Fig.(5).**

When measuring the diameter of the steam drops in the nozzle (N2A) at a pressure ratio of ( $\epsilon_o = 0.54$ ) at different values of moisture ratio, it is obtained that the diameter of the steam drops is within ( $40-110\mu\text{m}$ ) according to the variation of the moisture ratio that exists between ( $Y_o = 4.6\%, 6.8\%, 9.75\%$ ), as shown in **Fig. (6)**. The initial value of the moisture ratio leads to real change in diameter of drops at initial value of moisture, a great difference in diameter of drops is in a position after the exit section of nozzle, assuming that there is a sudden diverging after exit section of nozzle resulting in coagulation process at that zone. When measuring the diameter of the steam drops in the (N3A) at moisture ratio of ( $Y_o = 6.8\%$ ) and different values of pressure ratio, it is found that the diameter of the steam drops locates within ( $55-110\mu\text{m}$ ) according to the change of the pressure ratio that exists between ( $\epsilon_a = 0.54, 0.60, 0.66,$  and  $0.74$ ), see **Fig. (7)**. The geometry of nozzle has a great influence on the diameter of drops in the convergent part ( $r=50\mu\text{m}$ ). And, in the divergent part, the big increase in the diameter of drops and the increase of the pressure ratio lead to increase the diameter of drops along the x-axis with a little effect of initial values of moisture. In general, the thermodynamic parameters (pressure and temperature) had highest impact on drop diameter.

The calculations were achieved by a special computer program which illustrates the shown figures (figures that indicate the distribution of the diameter of the drops along the longitudinal axis of the channel) which were utilized to calculate the diameter of the steam drops.

### Drop Diameter Model

The average responses obtained for drop diameter were used in calculating the model of the response surface using the least-square method. For drop diameter prediction model, a reduced cubic model in coded terms was analyzed with backward eliminations regression of insignificant coefficients at an exit threshold of  $\alpha = 0.1$  in order to achieve a robust model. Some coefficients were removed, since they were aliased and not fitted for back elimination. The terms removed were ABC,  $B^2$ ,  $A^2C$ , C (light intensity), BC, AC,  $A^2B$ ,  $A^2$ , while the other terms and cubic ones were found aliased by the stepwise regression. Also, some terms were reinserted in order to preserve the hierarchy and allow for obtaining a formula with the actual factors rather

than coded ones. The terms that were reinserted were C, B<sup>2</sup>. Therefore, the only significant terms of the drop diameter model were A (pressure ratio), B (moisture ratio), AB (interaction between pressure ratio and moisture ratio), C<sup>2</sup>, AB<sup>2</sup>, in addition to the intercept. This means that the light intensity factor (term C) had no significant effect on the drop diameter values.

**Table 5** shows the analysis of variance produced by the software for the remaining terms. The model is significant at 95% confidence. It is noted that the squared term of moisture ratio is insignificant, while the independent effects of pressure ratio and moisture ratio, their interaction, the squared of light intensity as well as the interaction between the pressure ratio and square of moisture ratio are significant. The lack of fit test indicates a good model. The final drop diameter predicted model (equation) in terms of coded factor is:

$$\text{Drop Diameter} = +80.79 + 17.50 * A + 5.37 * B + 1.25 * C - 10.00 * A * B + 0.76 * B^2 + 3.63 * C^2 - 24.50 * A * B^2$$

And, the final predicted model (equation) in terms of actual factors, showing that the pressure ratio had the highest impact on the drop diameter, is

$$\begin{aligned} \text{Average Drop diameter } (\mu\text{m}) = & \\ & + 26501.75484 \\ & - 1.09295\text{E}+005 * \text{Pressure ratio} \\ & - 8550.20368 * \text{Moisture ratio} \\ & - 22.73393 * \text{Light intensity} \\ & + 35401.78571 * \text{Pressure ratio} * \text{Moisture ratio} \\ & + 660.64802 * \text{Moisture ratio}^2 \\ & + 3.63393 * \text{Light intensity}^2 \\ & - 2734.37500 * \text{Pressure ratio} * \text{Moisture ratio}^2 \end{aligned}$$

Looking at the normal probability plot (**Fig. 8**) or the drop diameter data, the residuals generally that falling on a straight line implying errors are normally distributed. Also, according to **Fig.9** that depicts the residuals versus predicted responses for drop diameter data, it is seen that no obvious patterns or unusual structure, implying models are accurate.

**Figure 10** reveals the contour graph of pressure ratio versus moisture ratio with drop diameter as a response, showing the interaction influence of both factors on drop diameter. Since the light intensity had no significant effect on the drop diameter, only two-factor interaction (2FI) is shown. It can be seen that for a constant intensity factor (3.30), the increase of pressure ratio from (0.59) to (0.69) resulted in an increase in the drop diameter (response) from (65)  $\mu\text{m}$  to more than (95)  $\mu\text{m}$ , when the moisture ratio increased from (5.2) to (7.6). But, when the moisture ratio is more than (7.6), the drop diameter increased to more than (95)  $\mu\text{m}$  at the lower pressure ratio (5.2) and then started to decrease up to (75)  $\mu\text{m}$  with increasing pressure ratio up to (0.69). Accordingly, the predicted model indicated that both pressure ratio and moisture ratio have a significant effect on drop diameter, but pressure ratio has the highest impact. Whereas, variation of the light intensity factor within the range (2.3-4.3) has insignificant influence on drop diameter, as illustrated in 2D plots in **Figs.(11)** and **(12)** for different values of moisture ratios and pressure ratios used in the present work.

The process of drop formation (or drop existence) in the two-phase flow is complicated. It can be said that the steam drop formation depends on the existence of small size nuclei which become the nucleus or core for steam drops. These nuclei may result in drops or decompose and disperse according to circumstances, such as pressure ratio, moisture ratio or effect of geometry. Also, during steam flow through the different channels, a collision occurs between the drops, resulting in drops coalescing or dispersion or deformation, and it could be all that.

The drop diameter of steam in apart close channels is much affected with pressure ratio ( $\epsilon_0$ ) variation and less influenced by the moisture ratio ( $Y_0$ ). For the limits taken in this study for ( $\epsilon_0$ ) within (0.59) and (0.69), one can find that the increase of drop diameter is between (65)  $\mu\text{m}$  and (95)  $\mu\text{m}$ , in proportion with the increase of ( $\epsilon_0$ ) value. Accordingly, this means that the effect of pressure ratio is an essential factor in the nature of the two-phase steam flow. Therefore, some of the primary values for the drop diameter can be determined. The influence of moisture ratio ( $Y_0$ ) that lies between (5.2) and (8.4), is less than the effect of ( $\epsilon_0$ ), where the steam drops that exist in the two-phase flow with a certain moisture ratio, contains basically an amount of drops with a certain size. The size of these drops, when passed through in apart close channels, may increase by a certain amount, and the ratio of increase is at a lower rate than that in the case of pressure variation ratio. The increase of drop diameter means the increase of the existed water volume in steam. Consequently, the results of this increase lead to reduce the efficiency of channels that work in these conditions in addition to increase of corrosion ratio caused by the moisture increase, particularly in the late stages of steam turbines.

Table (1) Basic design of three sizes of nozzles used in the experimental work

Nozzle (N)	$l_0$	$l_1$	$l_2$	$l_0/l_1$	$l_2/l_1$	$F^*/F_1$	M	$\epsilon_a$
1	140	87	53	1.59	0.59	0.767	1.63	0.240
2	140	61	79	2.29	1.29	0.763	1.602	0.245
3	180	65	115	2.76	1.78	0.787	1.63	0.245

Table 2: Input parameters used in the experimentation with respective coding

Parameter	Symbol	Level (Coding)		
		-1	0	+1
Pressure ratio	$\epsilon_0$	0.238	0.241	0.245
Moisture ratio	$Y_0$	5.2	6.8	8.4
Light intensity	$I_0$	2.3	3.3	4.3

**Table 3: Experimental design matrix in coded and actual factors**

Test Number	Run Number	Pressure ratio ( $\epsilon_0$ )		Moisture ratio ( $Y_0$ )		Light intensity ( $I_0$ )	
		Code	Value	Code	Value	Code	Value
		1	16	-1	0.238	-1	5.20
2	18	1	0.245	-1	5.20	-1	2.30
3	7	-1	0.238	1	8.40	-1	2.30
4	13	1	0.245	1	8.40	-1	2.30
5	5	-1	0.238	-1	5.20	1	4.30
6	2	1	0.245	-1	5.20	1	4.30
7	4	-1	0.238	1	8.40	1	4.30
8	3	1	0.245	1	8.40	1	4.30
9	12	-2	0.234	0	6.80	0	3.30
10	19	2	0.249	0	6.80	0	3.30
11	10	0	0.241	-2	3.60	0	3.30
12	6	0	0.241	2	10.00	0	3.30
13	14	0	0.241	0	6.80	-2	1.30
14	1	0	0.241	0	6.80	2	5.30
15	9	0	0.241	0	6.80	0	3.30
16	17	0	0.241	0	6.80	0	3.30
17	20	0	0.241	0	6.80	0	3.30
18	8	0	0.241	0	6.80	0	3.30
19	15	0	0.241	0	6.80	0	3.30
20	11	0	0.241	0	6.80	0	3.30

**Table 4: Experimental design matrix used for input parameters in terms of actual factors with the experimental values of average drop diameter.**

Test No.	Run No.	Type of point	Pressure ratio ( $\epsilon_0$ )	Moisture ratio ( $Y_0$ )	Light intensity ( $I_0$ )	Average Drop diameter ( $\mu\text{m}$ )
1	16	Factorial	0.238	5.20	2.30	70
2	18	Factorial	0.245	5.20	2.30	82
3	7	Factorial	0.238	8.40	2.30	110
4	13	Factorial	0.245	8.40	2.30	80
5	5	Factorial	0.238	5.20	4.30	80
6	2	Factorial	0.245	5.20	4.30	80
7	4	Factorial	0.238	8.40	4.30	110
8	3	Factorial	0.245	8.40	4.30	72
9	12	Axial	0.234	6.80	3.30	40
10	19	Axial	0.249	6.80	3.30	110
11	10	Axial	0.241	3.60	3.30	77
12	6	Axial	0.241	10.00	3.30	90
13	14	Axial	0.241	6.80	1.30	90
14	1	Axial	0.241	6.80	5.30	100
15	9	Center	0.241	6.80	3.30	80
16	17	Center	0.241	6.80	3.30	75
17	20	Center	0.241	6.80	3.30	85
18	8	Center	0.241	6.80	3.30	90
19	15	Center	0.241	6.80	3.30	70
20	11	Center	0.241	6.80	3.30	95

Table 5: Analysis of variance (ANOVA) for response surface reduced cubic drop diameter.

Source	Sum of squares	df	Mean square	F value	p-value Prob > F
Model	4477.63	7	639.66	10.89	0.0002 significant
A-Pressure ratio	2450.00	1	2450.00	41.73	< 0.0001
B-Moisture raatio	462.25	1	462.25	7.87	< 0.0159
C-Light intensity	25.00	1	25.00	0.43	0.5264
AB	800.00	1	800.00	13.63	< 0.0013
B <sup>2</sup>	15.18	1	15.18	0.26	0.6204
C <sup>2</sup>	348.00	1	348.00	5.93	0.0315
AB <sup>2</sup>	2401.00	1	2401.00	40.89	< 0.0001
Residual	704.57	12	58.71		
Lack of Fit	267.07	7	38.15	0.44	0.8454 not significant
Purr Error	437.50	5	87.50		
Core Total	5182.20	19			
Std. Dev.	7.66		R-Squared	0.8640	
Mean	84.30		Adj R-Squared	0.7847	
C.V. %	9.09		Pred R-Squared	0.6357	
PRESS	1888.04		Adeq Precision	14.444	



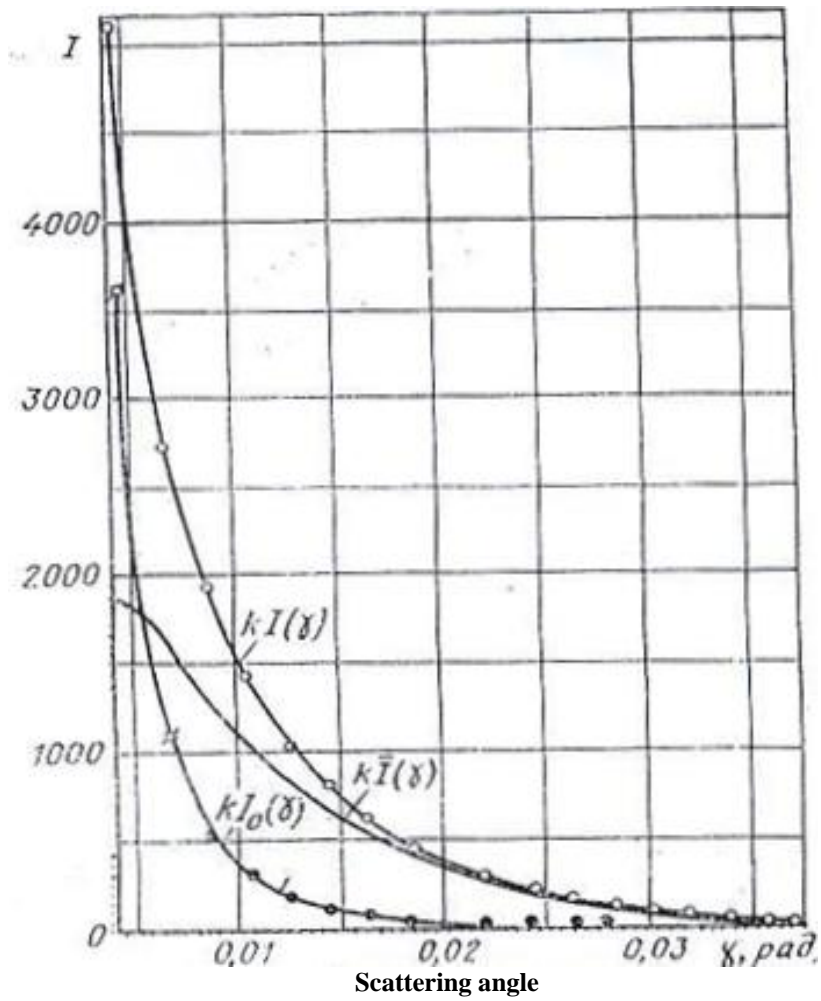


Fig.(1) Light intensity (I) scattering at small angles.

$KI_0(\gamma)$  = Scattering in air,  $KI(\gamma)$  = Scattering with steam existence,  $KI(\gamma) = I - I_0$

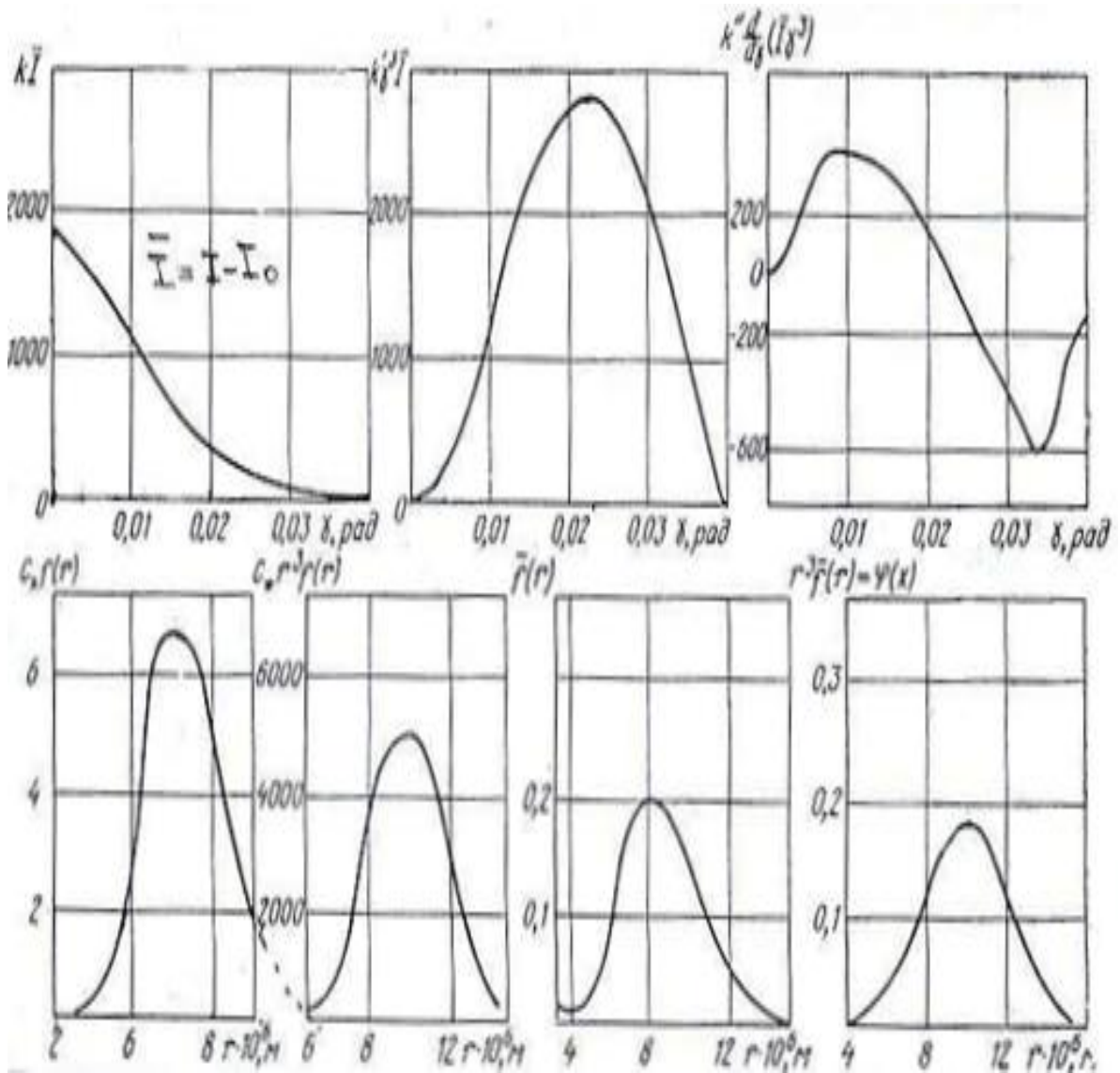


Fig.(2) Steam droplets distribution (According to size).

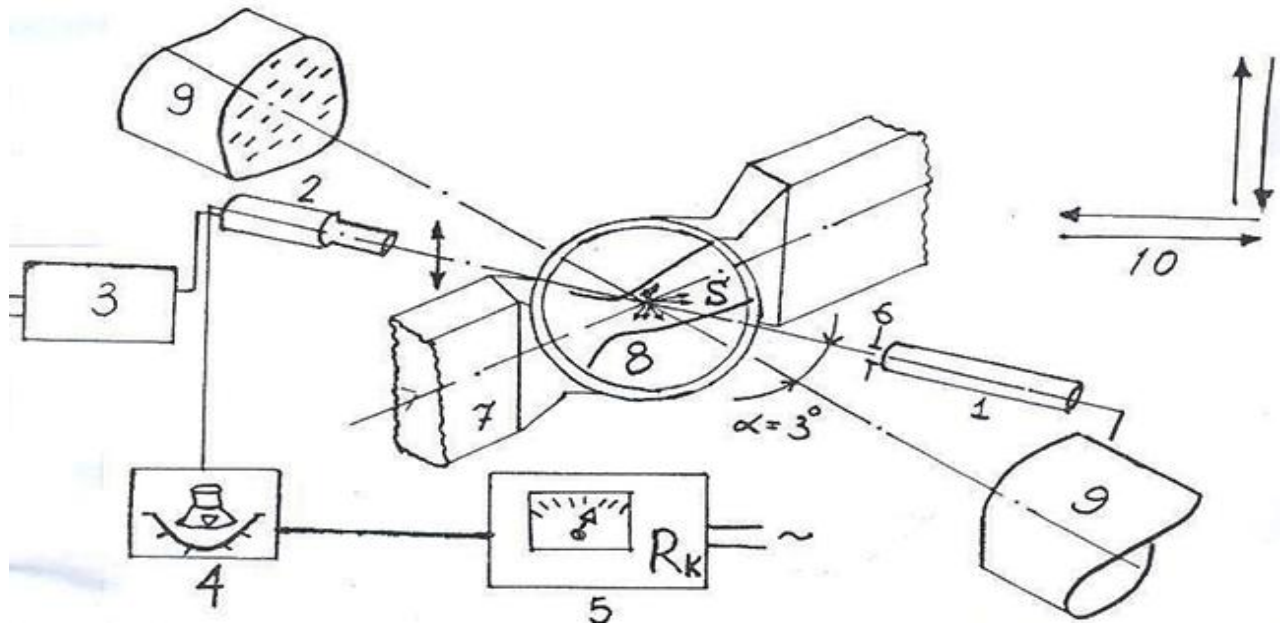


Fig.(3) Schematic diagram for the light scattering plant.

- |   |                                     |   |
|---|-------------------------------------|---|
| 1-Laser light source with continuous ray  | 2-Photoelectric cells               | 3-High voltage source                                   |
| 4-Microampere                             | 5- Indicator                        | 6- Variable opening                                     |
| 7- Working body                           | 8- The investigated channel (model) | 9-Tiber's device to photograph the current spectrometer |
| 10-Mechanical device to control the plant |                                     |   |

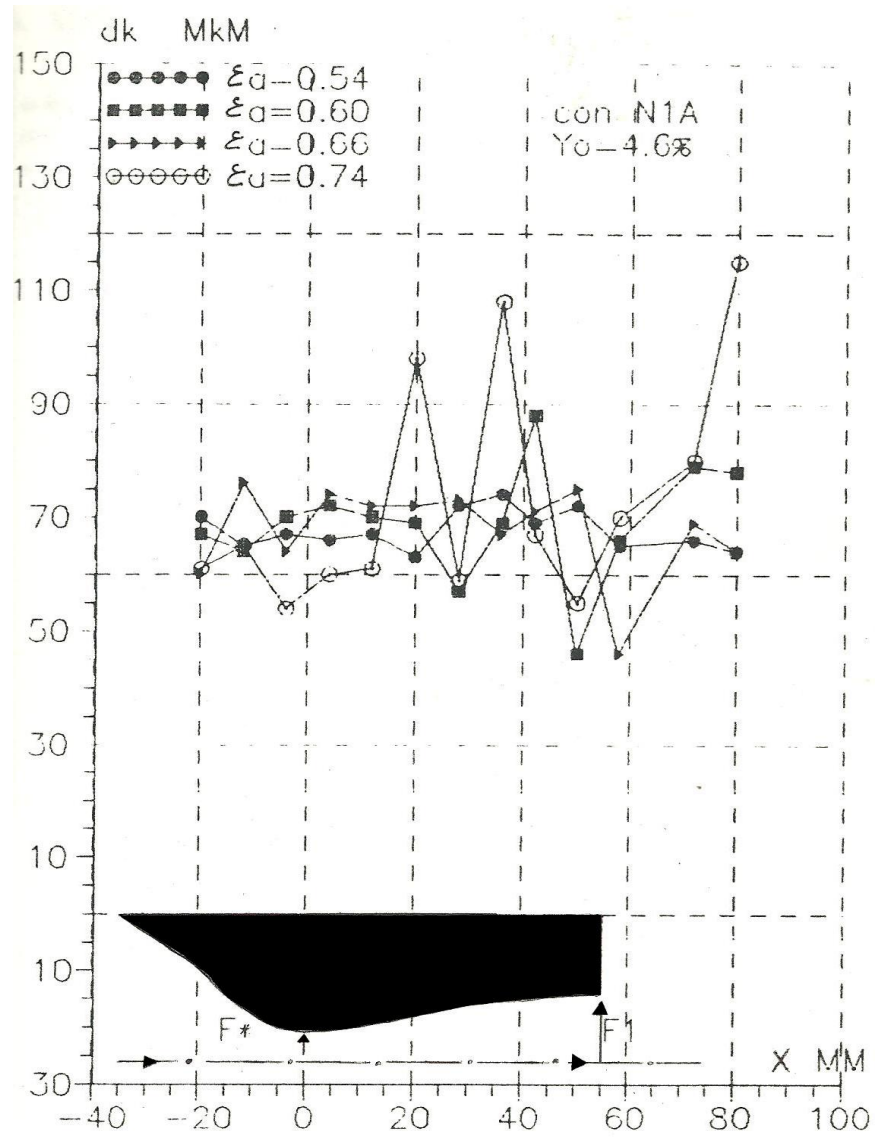
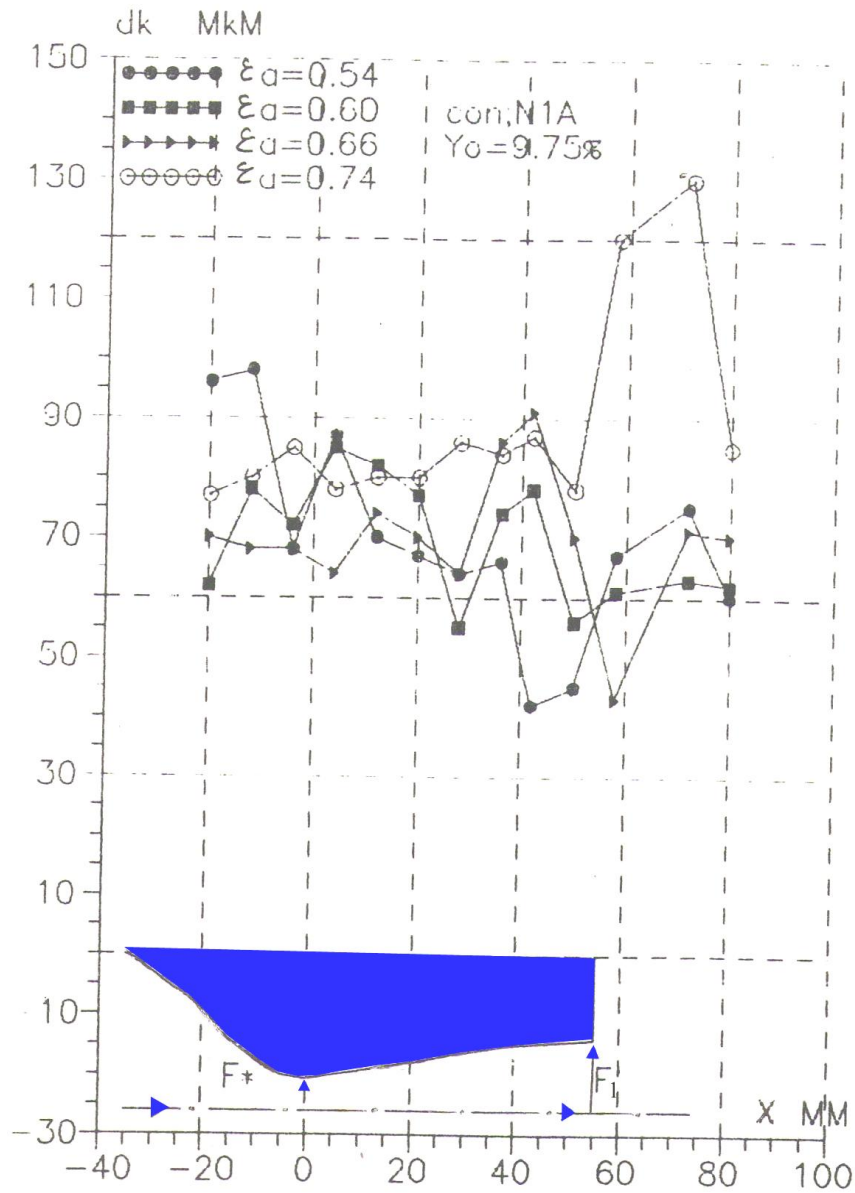
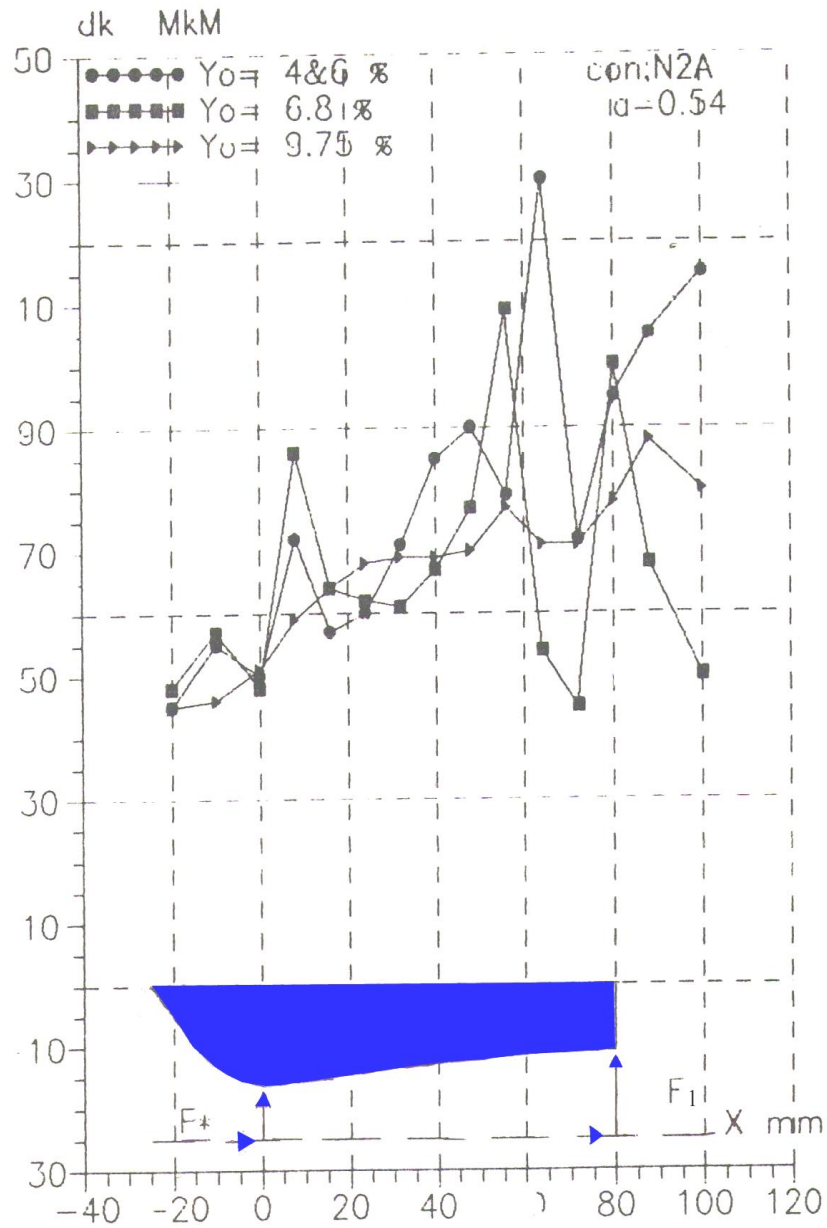


Fig.(4) Distribution of dispersed droplets along the longitudinal axis of Laval channel N1A at different pressure ratios ( $\epsilon_0$ ) and constant relative moisture ( $Y_0$ ) of 4.6%.



**Fig.(5) Distribution of dispersed droplets along the longitudinal axis of Laval channel N1A at different pressure ratios ( $\epsilon_o$ ) and constant relative moisture ( $Y_o$ ) of 9.75%.**



**Fig.(6) Distribution of dispersed droplets along the longitudinal axis of Laval channel N2A at different moisture ratios ( $Y_0$ ) and constant pressure ratio ( $\epsilon_0$ ) of 0.54.**

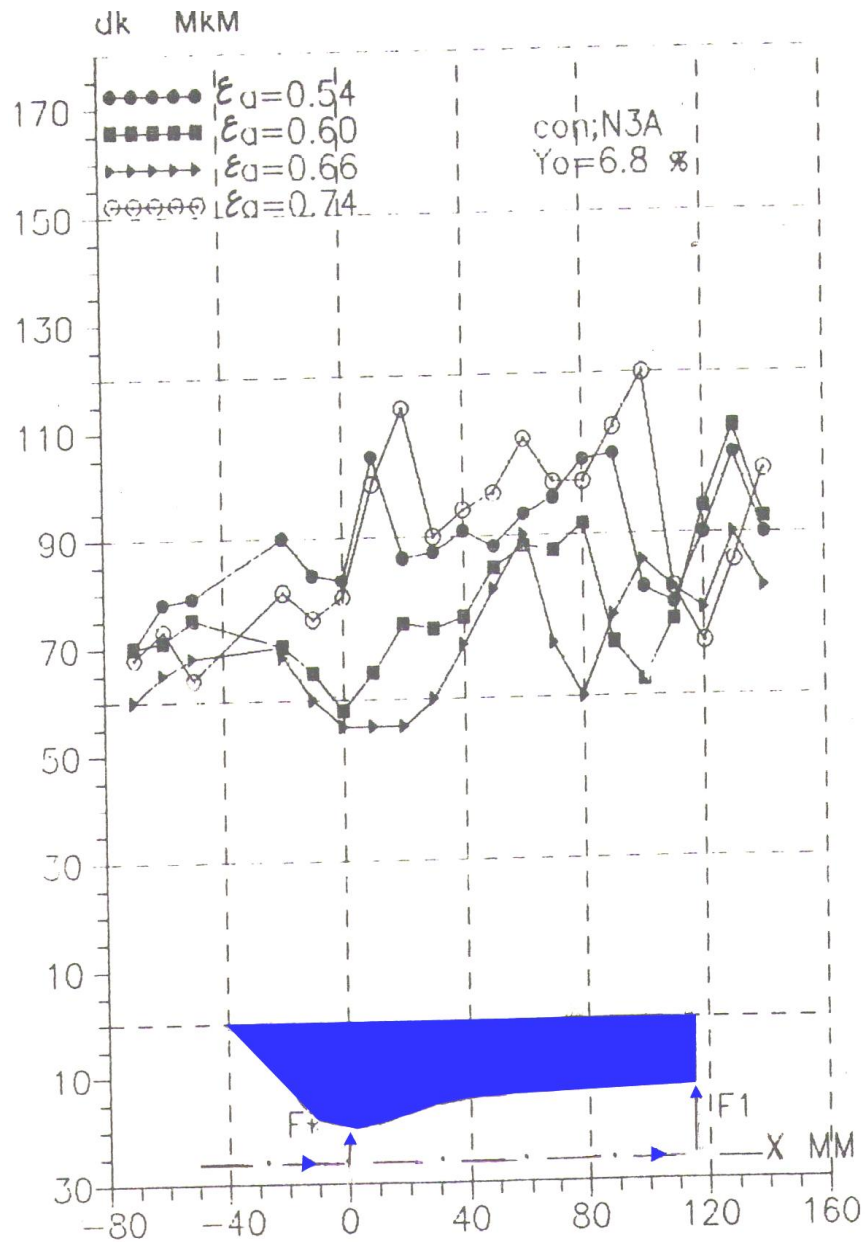


**Fig.(7) Distribution of dispersed droplets along the longitudinal axis of Laval channel N3A at different pressure ratios ( $\epsilon_0$ ) and constant moisture ratio ( $Y_0$ ) of 6.8%.**



Design-Expert® Software  
Drop Diameter

Color points by value of  
Drop Diameter:

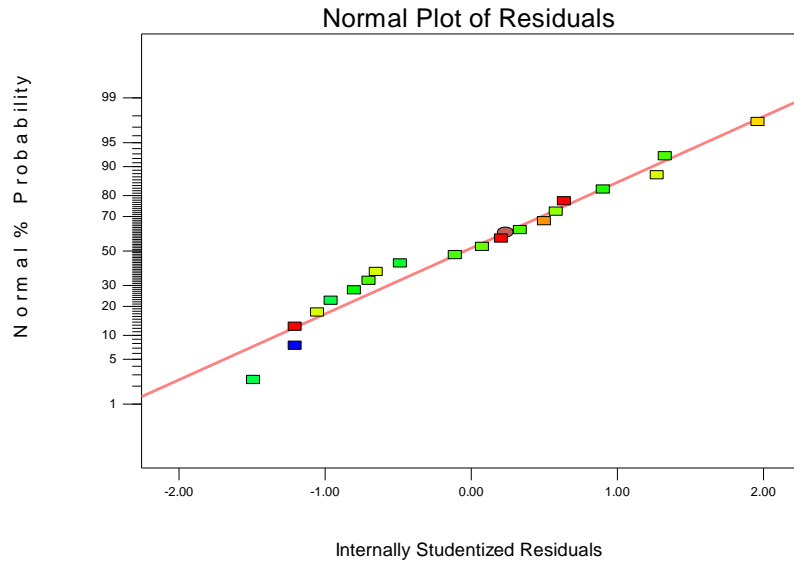


Fig.(8) Normal probability plot of residuals for drop diameter data.

Design-Expert® Software  
Drop Diameter

Color points by value of  
Drop Diameter:

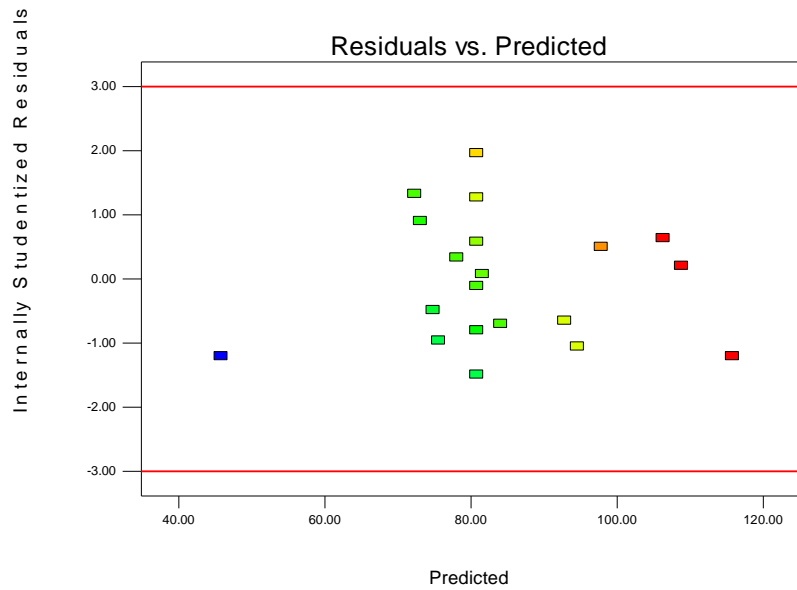
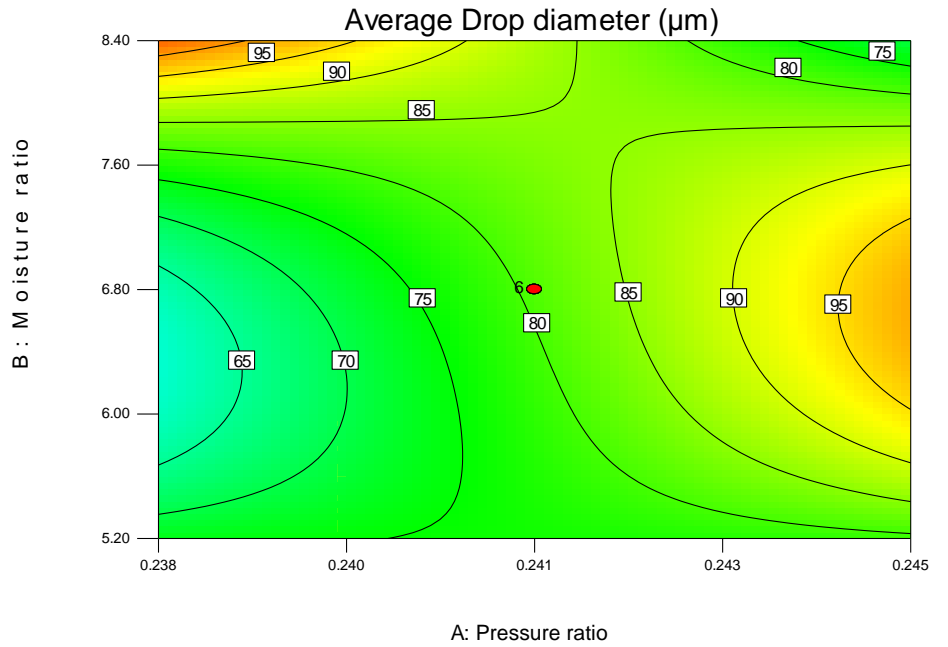


Fig.(9) Residual versus predicted responses for drop diameter data.

Design-Expert® Software  
 Factor Coding: Actual  
 Average Drop diameter (µm)  
 ● Design Points  
 110  
 40  
 X1 = A: Pressure ratio  
 X2 = B: Moisture ratio  
 Actual Factor  
 C: Light intensity = 3.30



**Fig.(10) Contour graph of drop diameter as a function of pressure ratio and moisture ratio, showing the interaction effect of both factors on drop diameter**

Design-Expert® Software  
 Factor Coding: Actual  
 Average Drop diameter (µm)  
 --- CI Bands  
 X1 = C: Light intensity  
 Actual Factors  
 A: Pressure ratio = 0.241  
 B: Moisture ratio = 8.40

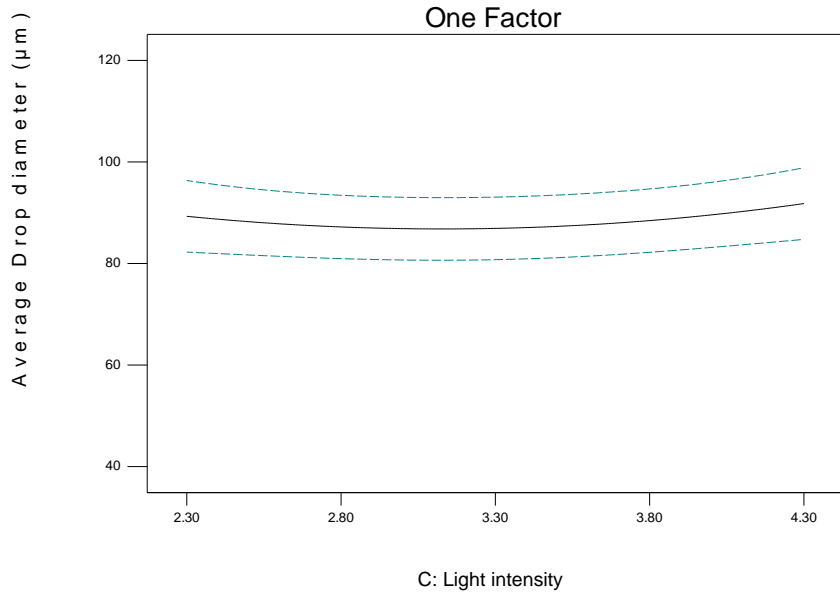


**Fig.(11) 2D plot showing the effect of light intensity on drop diameter at pressure ratio = 0.241 and moisture ratio = 8.40**

Design-Expert® Software  
 Factor Coding: Actual  
 Average Drop diameter (µm)  
 --- CI Bands  
 X1 = C: Light intensity  
 Actual Factors  
 A: Pressure ratio = 0.245  
 B: Moisture ratio = 6.80

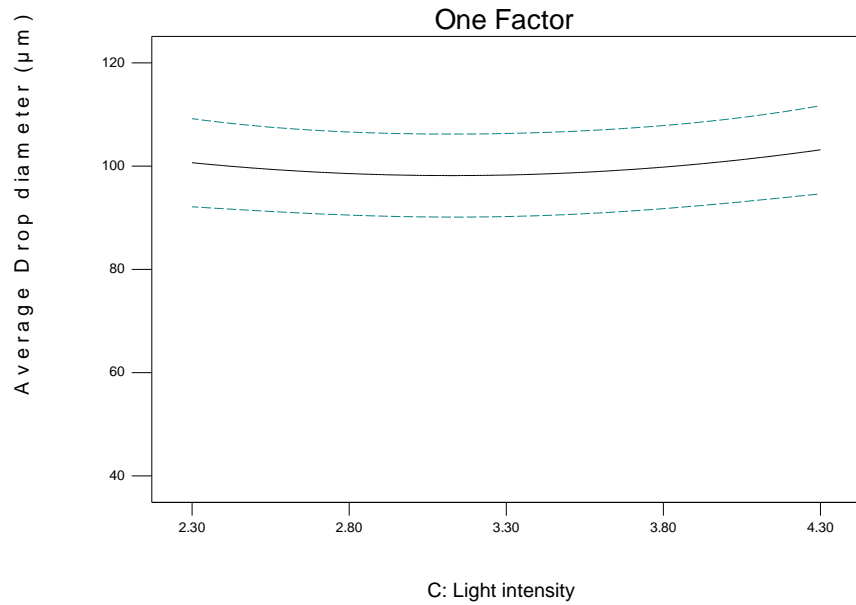


**Fig.(12) 2D plot showing the effect of light intensity on drop diameter at pressure ratio = 0.245 and moisture ratio = 6.80.**

## CONCLUSIONS

The experimental results in Laval channels during the flowing of the moistured steam permits to predict the followings:

- 1- By using the small angles method in case of flowing of a steam of two-phase inside the Laval channel, the calculated diameter of the drops of the condensed steam along the longitudinal axis of the channel varies between (40-110µm) according to the pressure ratio change. Also, the diameter of the steam drops is within (40-110µm) according to the variation of the moisture ratio, where the error is not more than (26%).
- 2- Using the small angles method allows to clarify actually the study of composition of the nature of the dispersed case of the flowing steam (two-phase) within the investigated values of the moisture ratio and pressure (moisture and pressure values).
- 3- The geometry of Laval Nozzle has a great influence on the nature of the flowing steam through the channel (diameter of drops, compressive shock). And, the channels are used with the engineering specifications indicated in **Table (1)**.
- 4- The predicted model indicated that that both pressure ratio and moisture ratio have a significant effect on drop diameter, but pressure ratio has the highest impact. Whereas, variation of the light intensity factor within the range (2.3-4.3) has insignificant influence on drop diameter.

## REFERENCES

- [1] Tatsuno, K., "Water Droplet Size measurements in an Experimental Steam Turbine Using an Optical Fiber Droplet Sizer", Center Toshiba Corporation, Kawsaki, Japan, *Journal of Heat Transfer*, November, vol. 10/93, 1986.
- [2] Walter, P. T. and Skingley, P. C., "An Optical Instrument for Measuring the Wetness Fraction and Droplet Size of Wet Steam Flows in LP Turbine", *Inst. Mech. Engrs.*, C14/79, 1979.
- [3] Kantola, R. A., "Condensation in Steam Turbines", *EPRI*, CS-2528 RP, 735-1 Aug., 1982.
- [4] Ederhof, A. and Dibelius, G., "Determination of Droplet Size and Wetness Fraction in Two-Phase-Flows Using a light scattering Technique", *Sixth Thermodynamics and Fluid Mechanics convention, I. Mech. E.*, C50/76, 1976.
- [5] Montgomery, D. C., "Design and Analysis of Experiments", 5<sup>th</sup> Edition, John Wiley & Sons Inc., 2001.
- [6] Montgomery, D. C., "Design and Analysis of Experiments: Response surface method and designs", New Jersey: John Wiley and Sons, Inc., 2005.
- [7] Aggarwal, A., and Singh, H., "Optimization Techniques - A retrospective and Literature Review", *Sadhana*, vol.30, Part 6, pp. 699-711, 2005.
- [8] Hiroyki Kawagish, Akihiro Onoda, Naoki Shibukawa and Yoshiki Niizeki, "Development of Moisture Loss Models in Steam Turbine", *Heat Transfer –Asian Research*, Article Published on line, 27 Dec, 2011, DOI.10.1002/hti 20395.
- [9] A. G. Gerber and A. Mousavi, "Representing Polydispersed Droplet Behavior Nucleating Steam Flow", *Journal of Fluid Engineering*, 2007- link.aip.org.
- [10] White, A. J., "A comparison of modeling Methods for Polydispersed Wet-Steam", *International Journal of Numerical Methods in Engineering*, Vol. 57, Issue 6, pp. 819-834, June 2003.
- [11] A. G. Gerber, "Two-Phase Eulerian / Lagrangian Model for Nucleating Steam Flow", *Journal of Fluids Engineering*, 2002, link.aip.org.
- [12] Bank, S. J. et. al., "A Laser Diagnostic Technique for the Measurement of Droplet and Particle Size Distribution", University of Sheffield, Department of Chemical Engineering and Fuel Technology in Sheffield Open Library OL20689636M, October 29, 2008.
- [13] Marchetti, J. M. and Svenden, H. F., "Improvements on a Laser Scattering Technique for Droplet Size Measurement Applied to Gas-Liquid Separation Equipment", *Measurement*, Vol. 17, Issue 2, pp. 493-499, Feb. 2011.
- [14] Giordano, M., Hercus, S. J. and Cinella, P., "Effects of Modeling Uncertainties in Condensing Wet-Steam Flows Through Supersonic Nozzles", V European Conference on Computational Fluid Dynamics, ECCOMAS CFD 2010, J. C. F. Pereira and A. Sequerira (Eds), Lisbon, Portugal, 14-17 June, pp. 1-20, 2010.
- [15] Mahpeylcar, M. R. and Amirirad, E., "Suppression of Condensation Shock in Wet Steam Flow by Injection of Water Droplets in Different Regions of a Laval nozzle", *Transaction B: Mechanical Engineering*, Vol. 17, No. 5, pp. 337-347, 2010.

[16] Wroblewski, W., Dykas, S. and Gepert, A., “Steam Condensing Flow Modeling in Turbine Channels”, Institute of Power Engineering and Turbomachinery, Silesia University of Technology, Konarskiego 18, 44100 Gliwice, Poland, 2009.

[17] Mohsin, R. and Majidm Z. A., “Water Condensation in Low Pressure Steeam Turbine: A Nucleation Theory- part II, J. of Chemical and Natural Resources Engineering, Special Edition, pp. 50-63, 2008.

[18] Avetissian, A. R., Philppov, G. A. and Zaichik, L. I., “Effects of turbulence and Inlet Moisture on Two-Phase spontaneously Condensing Flows in Transonic Nozzles”, International J. of Heat and mass Transfer, 51, pp. 4195-4203, 2008.

## Nomenclature of Nozzle

P = Presser, bar

$\epsilon_o = P/P_o$  = Pressure ratio with initial values

$\epsilon_a = P_a/P_o$  = Pressure ratio at any point along the x-axis of nozzle

M = Mach number

M1t = Mach theoretical

$P_a$  = Pressure for any point along the nozzle, bar

$P_o$  = Initial pressure, bar

$T_o$  = Initial temperature, k

$Y_o$  = Humidity, %

$l_o$  = Length of nozzle, mm

$l_1$  = Length of convergent part, mm

$l_2$  = Length of divergent part, mm.

$F_2$  = exit area, mm.

$F^*$  = Critical area, mm.

$I(\chi)$  = Scattered light intensity pattern measured droplets, W.

$I(r,\chi)$  = Scattered light intensity by diameter droplet, W...

m = Refractive index (m=1.33 for water).

$n(r)$  = Droplet size distribution

$\lambda$  = Light wavelength, mm.

r = Drop diameter,  $\mu$ m.